XVII IMEKO World Congress
Metrology in the 3rd Millennium
June 22–27, 2003, Dubrovnik, Croatia

INERTIAL GRADE LASER ACCELEROMETER-PRACTICABILITY AND BASIC EXPERIMENTS

Wolfgang Holzapfel, Nejat Mahdavi, Martin Suske

University of Kassel, Institute of Measurement and Automation, D-34109 Kassel, Germany

Abstract – A novel laser accelerometer is introduced, its physical principle and main characteristics are explained, and preliminary experimental results are presented. The accelerometer utilizes two Nd:YAG laser crystals and a common proof mass which operate in push-pull mode. The main advantages of the described laser accelerometer are wide measuring range which covers 9 decades up to 100 m/s², very high linearity over measuring range and excellent dynamics (20 kHz bandwidth). In comparison to servo accelerometers, these results represent a high-performance sensor. The measurement uncertainty and precision analysis have been carried out according to GUM guidelines. The analysis shows that the relative uncertainty in sensitivity of the laser accelerometer amounts to 10^{-6}.

Keywords: Inertial Navigation, Photoelastic Effect, Laser Accelerometer.

1. INTRODUCTION

In recent decades the demand on high performance inertial accelerometer sensors has drastically increased. Precision measurement of acceleration and inertial forces is a common requirement in measurement technology, e.g. in the field of gravimetric/seismic measurements, in the determination of vibrations in buildings, industrial robot navigation or in vehicle guidance and navigation. Especially for inertial guidance of aerospace vehicles, highly accurate and sensitive on-board accelerometers are used to determine position and speed of the vehicle [1], [2].

In conventional closed-loop accelerometers as well as in silicon bulk-micromachined accelerometers, the inertial force is balanced by opposing spring force and deflection of the mass is a measure of acceleration. The deflection is determined by capacitive, piezoelectric or piezo-resistive principles. In such accelerometers, increasing static sensitivity by increasing proof mass or decreasing spring stiffness is associated with decreasing bandwidth.

Investigations in the field of optics reveal that the photoelastic effect can be used in high-resolution force and acceleration measurements [3], [4]. In [5] a photoelastic accelerometer is developed, however with narrow measuring range and bandwidth. In the present work, we introduce a novel accelerometer using the photoelasticity principle to affect the laser frequency. This approach leads to very wide measuring range, wide bandwidth and high resolution. This accelerometer is a potential high-accurate measuring device and because of its differential operation it is able to eliminate significant parts of measurement noise.

2. BASIC CONFIGURATION OF THE LASER ACCELEROMETER

Our contribution covers a new type of accelerometer operating on the base of Newton's axioms and utilizing high-precision force-to-frequency conversion by lasers. The physical principle of the laser force transducer is explained in [3], [4].

The basic structure of the inertial laser accelerometer consists of a proof mass which is supported between (two or more) photoelastic microlaser sensors all clamped in a small but solid housing as depicted in Fig. 1. The applied laser sensors are Nd:YAG crystals, their wavelength is $\lambda = 1064$ nm. With a proof mass of $M_0 = 1$ g, the accelerometer is a cube with an edge length of 10 mm. The housing is preloaded with a force F_0, which acts equally on both laser sensors. The construction of the accelerometer is a differential configuration, that is the force acting on one laser sensor due to acceleration *a* leads to increasing force F_0 and at the same time to decreasing force F_0 acting on the other laser sensor:

$$F_1(t) = F_0 + F_{a1}(t)$$
$$F_2(t) = F_0 - F_{a2}(t) \quad (1)$$

where $F_{a1}(t)$ and $F_{a2}(t)$ are inertial forces affecting on laser crystals due to acceleration *a*. In order to increase the shock resistance of the accelerometer in cross directions, the proof mass is fixed in the housing using parallel guides with high stiffness in cross direction and low stiffness in measuring direction as shown in Fig. 1.

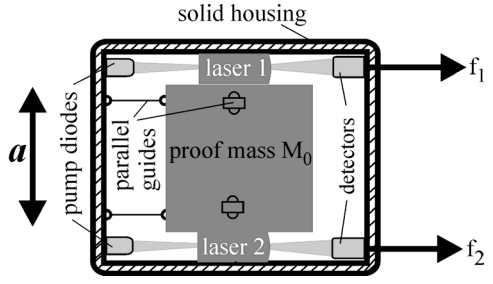

Fig.1. Basic configuration of the laser accelerometer

The direction of the input axis of the laser accelerometer is normal to the optical axes of the lasers. The photoelastic microlaser sensors act as force-tuned optical oscillators, which are supplied with pump diodes [3], [6]. Thus, the frequency-analogue output signal of each microlaser depends on the internal force F_{sens} produced by the common proof mass if the housing is accelerated. The optical difference frequency of the laser is then easily converted into an electrical beat signal of the same frequency f by a simple pin-diode/polarizer combination (detector) as:

$$f = f_0 + \frac{GC_0\nu}{nLD} F_{sens}(t) = f_0 + S_0 \cdot F_{sens}(t) \qquad (2)$$

with

$S_0 = \frac{GC_0\nu}{nLD}$ force sensitivity of the laser crystal

f_0 = offset beat frequency
C_0 = photoelastic constant
D = ∅ of laser crystal
n = refractive index of crystal
G = geometry factor
ν = light frequency
L = geometric length of crystal
F_{sens} = force detected by crystal

The last equation shows that the frequency deviation is inversely proportional to the laser dimensions, i.e. small geometry leads to a big sensitivity factor, which does not apply to conventional accelerometers.

3. DYNAMIC MODELING AND SIMULATIONS

The dynamic model of the accelerometer is depicted in Fig. 2. M_0 represents the proof mass and M_1 and M_2 are masses of laser crystals. Due to symmetrical construction of the device, damping *d* and stiffness *k* for both parts of the accelerometer are of the same magnitude.

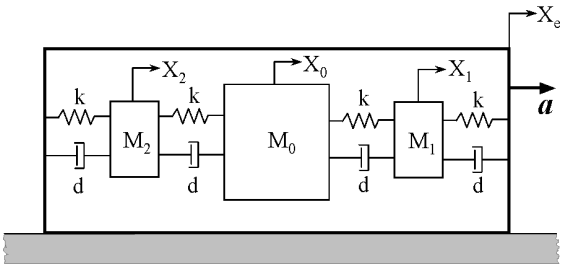

Fig.2. Dynamic model of the differential accelerometer
M_0: proof Mass, M_1 and M_2: laser crystals

For the parameters of the mathematical model the following values are used:
The proof mass can be selected for various measuring ranges. For a maximum input acceleration of 100 m/s² the corresponding proof mass is M_0 = 10 g which induces the force F_a= 0.5 N on each laser crystal. We assume the maximum frequency f_{max} measured by commercial frequency-measuring devices is 1.5 GHz. Due to the differential configuration of the accelerometer, the offset frequency f_0 shall be equal to $0.5 \cdot f_{max}$ i.e. 750 MHz. Under this assumption the required force sensitivity of the laser crystal is S_0=1.5 GHz/N. By using (2) and substituting the values $C_0=1.25\cdot10^{-6}$ mm²/N, n =1.82, $\nu=2.82\cdot10^{14}$ Hz and $G=8/\pi$ [7], the product L·D of the laser crystal is calculated $L\cdot D=0.32$ mm². The best choice is the diameter D=0.4 mm and the length L=0.8 mm which guarantees a longitudinal single mode activity of the laser. The density of the Nd:YAG crystal is ρ = 4.56 g/cm³, so their masses are $M_1=M_2=4.58$ mg.

The damping factor *d* is determined experimentally as d = 10 Ns/m. The stiffness *k* is due to the Hertz contact of the laser crystals located between the proof mass and the accelerometer housing which have the same material specifications. By using the calculation of Hertz, the resulting stiffness including the crystal stiffness is calculated $k = 5.0\cdot10^7$ N/m [6].

The dynamic equations are derived as follows. For mass M_1, M_0 and M_2 the 2. Newton axiom yields

$$\begin{aligned} &M_1(\ddot{x}_1 + \ddot{x}_e) + d\dot{x}_1 + kx_1 + d(\dot{x}_1 - \dot{x}_0) + k(x_1 - x_0) = 0 \\ &M_0(\ddot{x}_0 + \ddot{x}_e) + d(\dot{x}_0 - \dot{x}_2) + k(x_0 - x_2) + d(\dot{x}_0 - \dot{x}_1) + k(x_0 - x_1) = 0 \\ &M_2(\ddot{x}_2 + \ddot{x}_e) + d\dot{x}_2 + kx_2 + d(\dot{x}_2 - \dot{x}_0) + k(x_2 - x_0) = 0 \end{aligned} \qquad (3)$$

These three equations describe the dynamics of the sensor completely. The forces affecting on the laser sensors caused by the acceleration *a* as indicated in Fig. 2 are:

$$\begin{aligned} F_{a1} &= d(\dot{x}_0 - \dot{x}_1) + k(x_0 - x_1) \\ F_{a2} &= d(\dot{x}_2 - \dot{x}_0) + k(x_2 - x_0) \end{aligned} \qquad (4)$$

Due to the preloaded accelerometer housing, the total force applied to each laser crystal is respectively:

$$\begin{aligned} F_1 &= F_0 + F_{a1} \\ F_2 &= F_0 - F_{a2} \end{aligned} \qquad (5)$$

These forces produce internal forces F_{sens1} and F_{sens2} in the laser crystals. According to the minimal configuration of the laser force sensor, these forces are obtained for each crystal as [6]:

$$G(s) = \frac{F_{sens}(s)}{F_i(s)} = \frac{\frac{m}{2}s^2 + ds + k}{ms^2 + ds + k} \quad \text{for } i = 1,2 \qquad (6)$$

Fig. 3 shows the block diagram of the accelerometer with differential configuration.

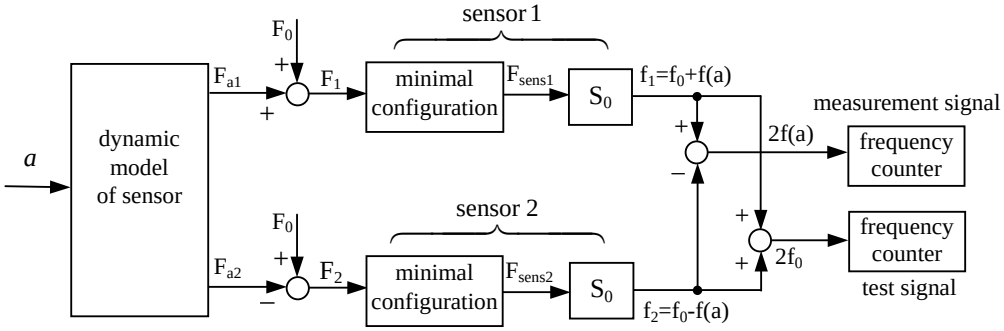

Fig. 3. Block diagram of the differential accelerometer including signal processing (full symmetry is assumed)

By using simulation techniques, the step response of the induced forces F_{sens1} and F_{sens2} as a result of input acceleration a = 10 m/s^2 are shown in Fig. 4. Owing to differential construction of the accelerometer the responses of the laser sensors are mirrored around the F_0 (here F_0=0.5 N) and are completely opposite in phase. For a proof mass of M_0=10 g, the settling time of the response is 7.8 ms and the resonance frequency is 11.3 kHz.

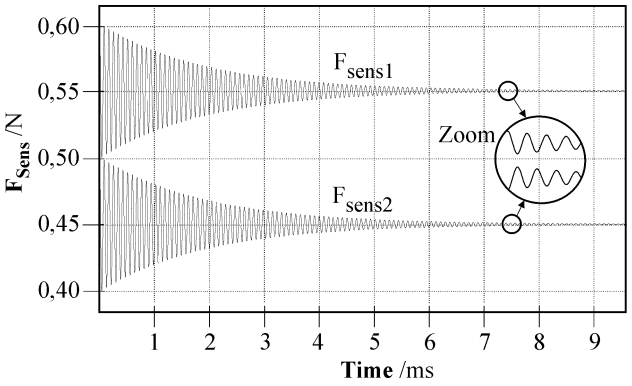

Fig. 4. Step response of the acceleration-induced forces F_{sens1} and F_{sens1} for an input acceleration a = 10 m/s^2 and S_0=1.5 GHz/N

In Fig. 5 the frequency responses $H(j\omega)=F_{sens}(j\omega)/a(j\omega)$ of the accelerometer for three different proof masses M_0 = 10 g, 2 g and 1 g are shown. The frequency responses include the dynamic model of the accelerometer (3) and the minimal configuration of the laser sensors (6).

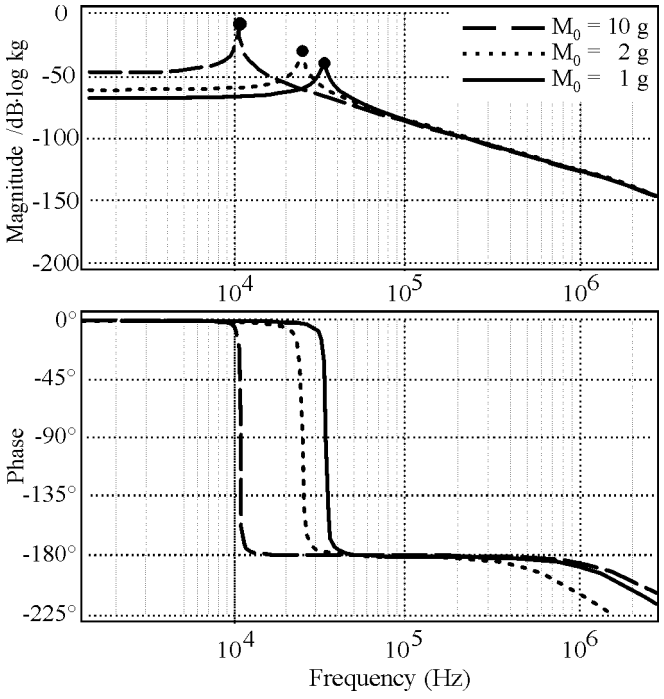

Fig. 5. Frequency response $H(j\omega)=F_{sens}(j\omega)/a(j\omega)$ of the accelerometer for different proof masses and S_0=1.5 GHz/N

The wide frequency response of the sensor is one of the outstanding features of the laser accelerometer. The figure shows that decreasing the weight of the proof mass leads to increasing the bandwidth and resonance frequency and decreasing the static gain $H_0=|H(\omega=0)|$ of the sensors. The latter, however, could be compensated by decreasing the laser crystal dimensions as pointed out in section 2.

4. SIGNAL PROCESSING IN THE ACCELEROMETER

As mentioned in section 1, the output signals of the accelerometer are electrical beat signals supplied by pin-diodes, their frequency is a function of acceleration:

$$\begin{aligned} f_1 &= f_{01} + E_0 \cdot F_{a1} = f_{01} + f_1(a) \\ f_2 &= f_{02} - E_0 \cdot F_{a2} = f_{02} - f_2(a) \end{aligned} \tag{7}$$

We assume that both laser crystals have exactly the same specifications, i.e. full symmetry in construction of the accelerometer is provided. In this case we have

$$\begin{aligned} f_{01} &= f_{02} = f_0 \\ |f_1(a)| &= |f_2(a)| = f(a) \end{aligned} \tag{8}$$

Subtracting the output signal of the pin diodes yields the desired measurement signal Δf as:

$$\Delta f(a) = f_1 - f_2 = 2f(a) = S \cdot a \tag{9}$$

which is a function of the applied acceleration a and is independent of the preload force F_0 and offset frequency f_0. $S=S_0H_0$ (in Hz/ms^{-2}) is called acceleration sensitivity. The advantage of the differential configuration beside increasing the sensitivity factor is to eliminate all common mode noises which may affect both laser sensors equally.

Another output signal can be generated by adding the output signal of the pin diodes as a test signal

$$\Sigma f = f_1 + f_2 = 2f_0 \tag{10}$$

This frequency signal is constant and completely independent of the inertial acceleration a and could be evaluated as a measure for symmetric operation of the laser sensors and accelerometer. It will remain constant during the measurement process if the accelerometer is operating properly. In Fig. 6 the results of simulations for both measurement signal Δf and test signal Σf are depicted. Due to the opposite phase of the $f_1(a)$ and $f_2(a)$, the test signal is an oscillation-free constant signal, its magnitude is $2f_0$.

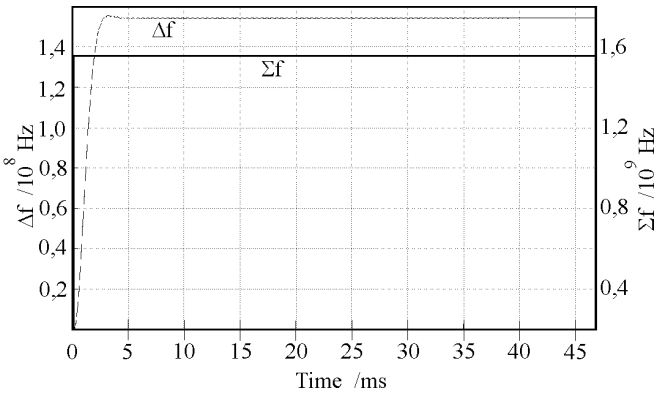

Fig. 6. Measurement and test signal as a result of input acceleration a=10 m/s² (M_0=10 g and S_0=1.5 GHz/N)

On the contrary, a transient oscillation of frequency 11.3 kHz appears in the measurement signal. These oscillations can be eliminated by using a proper low-pass filter allowing a measuring bandwidth of $0.6 \cdot f_{res.}$ in order to achieve an acceleration-dependent signal without distortion and oscillatory component.

In Table I the main features of the accelerometer for various proof masses and measuring ranges are shown.

Table I. Main characteristics of the accelerometer for various proof mass and constant size of crystals (S_0=1.5 GHz/N)

proof mass M_0	acceleration sensitivity S	measuring range	resonance frequency f_{res}
1 g	1.5 $\frac{\text{MHz}}{\text{m/s}^2}$	$10^{-6} \cdots 10^{3}$ m/s^2	35.6 kHz
2 g	3.0 $\frac{\text{MHz}}{\text{m/s}^2}$	$5 \cdot 10^{-7} \cdots 5 \cdot 10^{2}$ m/s^2	25.2 kHz
10 g	15.0 $\frac{\text{MHz}}{\text{m/s}^2}$	$10^{-7} \cdots 10^{2}$ m/s^2	11.3 kHz

5. ERROR ANALYSIS

Error analysis of the accelerometer is carried out according the ISO/BIPM *Guide to expression of Uncertainty in Measurement* (GUM). In this analysis, we assume full symmetry in construction of the accelerometer, thus frequency difference Δf doesn't depend on offset frequency f_0. The GUM is applied to investigate the uncertainty of the static accelerometer sensitivity. For this purpose, the possible uncertainties are categorized into the following contributions:

- uncertainty due to tolerances in the dimensions of laser crystal and proof mass, and crystal geometry
- uncertainty due to temperature deviations in environment and in accelerometer
- acceleration-induced uncertainty
- uncertainty in calibration process.

The mathematical expression for the output signal f according to (2) can be generally formulated as:

$$f = f(f_0, G, C_0, \nu, n, L, D, T) \tag{11}$$

where T is temperature and affects various parameters of *f*.

According to the GUM guidelines [8], the total expression for the measurement uncertainty is

$$u^2(f) = \Sigma[c_i u(x_i)]^2 + 2\Sigma\Sigma\,[c_i u(x_i) c_k u(x_k) r(x_i, x_k)] \tag{12}$$

where

$c_i = \partial f / \partial x_i$ the sensitivity coefficient of the measurement

$u(x_i) = \sqrt{\text{Var}[X_i]}$ the standard measurement uncertainty of variable x_i

$r(x_i, x_k)$ correlation coefficient of variables x_i and x_k

The results of uncertainty analysis considering geometrical tolerances arising in manufacturing, temperature deviations, acceleration-induced uncertainty and uncertainty in calibration process are summarized in Table II.

Table II. Uncertainty analysis of the sensitivity factor of laser accelerometer (M_0=10 g and S_0=1.5 GHz/N)

uncertainty source	uncertainty contribution / $\frac{\text{Hz}}{\text{m/s}^2}$	ratio of uncertainty to S_0
geometric tolerances	*7509.8*	*5.0 10^{-5}*
temperature	10839.5	7.2 10^{-6}
acceleration induced	9.1	6.1 10^{-9}
calibration with an accuracy of 10^{-3}	75.0	5.0 10^{-8}
total uncertainty (without geometric tolerances)	**10839.7**	**7.2 10^{-6}**

In the calculation of the total uncertainty, the contribution of the geometrical manufacturing tolerances is not considered because it can be eliminated during the calibration process. Analysis shows that the uncertainty due to the temperature fluctuations is the biggest uncertainty source, however, a major part of the temperature contribution to uncertainty can be compensated [9], so the relative uncertainty in sensitivity of the laser accelerometer amounts to 10^{-6}; i.e. deviation of internal parameters as well as environmental disturbances have little influence on the measurement results.

Another error source to be investigated is the effect of unsymmetrical operation of the accelerometer due to different specifications of the laser crystal and different temperature distribution (and gradient) in the accelerometer [9]. For this purpose, a block diagram is proposed in Fig. 7.

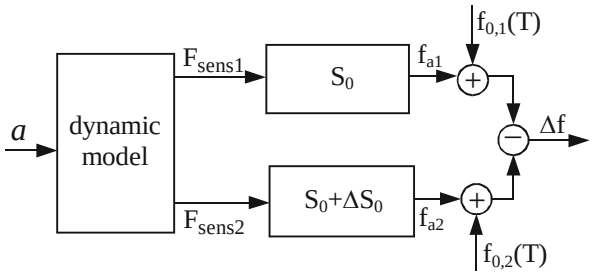

Fig. 7. Model for uncertainty caused by unsymmetrical operation of the accelerometer

According to this model, the measurement and test signals are:

$$\begin{aligned} \Delta f &= 2S_0F_a + \Delta f_0(T) + \Delta S_0F_a \\ \Sigma f &= 2f_0 + [\Delta f_{01}(T) + \Delta f_{02}(T)] + \Delta S_0F_a \end{aligned} \tag{13}$$

The last two terms in each equation represent the differences in offset frequencies and in static sensitivity factors of the laser crystals, respectively, which introduce additional uncertainty in the accelerometer. By advanced signal processing techniques and temperature sensing it is possible to reduce these error terms. The term $\Delta f_0(T)$ could be eliminated by a temperature compensation process, knowing the temperature of both laser crystals. The last term could be minimized by tight manufacturing tolerances. Further

analysis could be done to determine the effects of other environmental disturbances such as air pressure, external electric and magnetic fields, etc. which are not considered here. Our experiments show that these disturbances under normal environmental conditions have no effect on the frequency of laser crystals. Another disadvantage which the conventional accelerometers suffer from, is the so-called cross-axis sensitivity which in this accelerometer should be zero due to the differential configuration.

6. EXPERIMENTAL AND RESULTS

Our simulation results on differential laser accelerometer are supported by experimental data, which we gained in two areas:

1. Experiments covering precise force-to-frequency conversion by Nd:YAG laser crystal.
2. Experiments on drift suppression in the output channel of differential laser accelerometer.

Concerning 1, our experiments demonstrate that the photoelastic effect in diode-pumped small monolithic Nd:YAG lasers can be applied successfully to high precision force measurement. The measurement range of the laser force sensor covers 9 decades in which its output frequency is strictly proportional to the applied force magnitude with nonlinearity error and reproducibility of lower than 10^{-4}, creeping below 10^{-5} and hysteresis 10^{-4} [3], [6].

It is of interest here that force sensitivity S_0 actually increases strongly if the size of the laser crystals is miniaturized as in (2). Furthermore, an excellent dynamic response in force measurement is offered: based on the minimal configuration of the laser crystal (6), the modulating force is converted into frequency without any change in the conversion factor within the measurement bandwidth from DC to at least 100 kHz. The experiments show that the frequency of modal oscillations of the used laser crystal is in the range of 10^7-10^{10} Hz which is far from the resonance frequency of the accelerometer. The transient behaviour of the laser process is approximately 10^9-10^{10} Hz. This is again several times the resonance frequency of the accelerometer and hence no influence on the measurement process.

Concerning 2, the observed drift suppression in the output channel of differential laser accelerometer applying the photoelastic effect was in the order of $2.5 \cdot 10^{-3}$ which was observed over a period of several hours. Thus, the differential configuration actually offers a possibility to eliminate the common mode disturbances which may affect on laser crystals. This leads to long-term stability of the accelerometer operation.

7. CONCLUSIONS

Contrary to well known servo accelerometers, the measurement bandwidth of the laser accelerometer does not decrease if its measurement sensitivity and its resolution increases. According to Table I, by decreasing the proof mass, the bandwidth of the accelerometer could be increased. At the same time, increasing the measurement range is possible by decreasing the laser crystal dimensions. So a wide range of requirements in the field of acceleration measurement in the range of 9 decades within DC to 20 kHz frequency range will be covered by properly combining proof mass and laser crystal dimensions.

Thus, precise measurements of static acceleration and fast time-depending acceleration are feasible with high sensitivity and high resolution. Since some challenging application areas such as aerospace and aircraft inertial navigation demand extra precision accelerometers, we conclude that accelerometers applying microlaser technology can be practised offering inertial grade qualities. Further applications are vibration analysis, tactile robot sensing and high-precision measurements in machine tools.

REFERENCES

[1] A. Lawrence, "Modern Inertial Technology", *Springer-Verlag*, New York, 1993.

[2] S. Merhav, "Aerospace Sensor Systems and Applications", *Springer-Verlag*, New York, 1996.

[3] W. Holzapfel, M. Finnemann, "High-resolution force sensing by diode-pumped Nd:YAG lasers", *Optics Letters* 23, pp. 2062-2064 (1993)

[4] W. Holzapfel, W. Settgast, "Force to frequency conversion by intracavity photoelastic modulation", *Applied Optics*, 21, pp. 4585-4594 (1989)

[5] W. Su, J. A. Gilbert, M. D. Morrissey, Y. Song, "General-purpose photoelastic fibre optic accelerometer", *Opt. Eng.* vol. 36 No. 1, Jan. 1997.

[6] W. Holzapfel, St. Neuschaefer-Rube, M. Kobusch, "High-resolution, very broadband force measurements by solid-state laser transducers", *Measurement* 28, 4, pp. 277-291 (2000)

[7] W. Holzapfel, L. Hou, St. Neuschaefer-Rube, "Error Effects in Microlaser Sensors", Proceedings of XVI IMEKO World Congress, 2000, Vienna, Austria, Vol. III, pp. 85-90

[8] GUM, "Guide to expression of Uncertainty in Measurement", first edition, 1993, corrected and reprinted 1995, International Organization for standardization (Geneva, Switzerland)

[9] S. Neuschaefer-Rube, W. Holzapfel and L. Hou, "Signal properties of monolithic Nd:YAG lasers", Proceedings of XVI IMEKO World Congress, 2000, Vienna, Austria, Vol. II, pp. 243-248

Authors:

Prof. Dr.-Ing. Wolfgang Holzapfel, University of Kassel, Institute of Measurement and Automation, D-34109 Kassel, Germany, Fax: +49-561-8042847, E-mail: holzapfel@uni-kassel.de

Dipl.-Ing. Nejat Mahdavi, University of Kassel, Institute of Measurement and Automation, D-34109 Kassel, Germany, Fax: +49-561-8042847, E-mail: mahdavi@uni-kassel.de

Dipl.-Ing. Martin Suske, University of Kassel, Institute of Measurement and Automation, D-34109 Kassel, Germany, Fax: +49-561-8042847, E-mail: martin.suske@uni-kassel.de